Supplementary Information

Exposing (002) Active Facet by Reducing Surface Energy for High-Performance $Na_3V_2(PO_4)_2F_3$ Cathode

Zhuangzhi Li[a], Lang Qiu[a], Ping Li[a], Hao Liu[b], Dong Wang[c], Weibo Hua[d], Ting Chen[e], Yang Song[a, f], Fang Wan[a], Benhe Zhong[a], Zhenguo Wu*[a] and Xiaodong Guo*[a]

[a] School of Chemical Engineering, Sichuan University, Chengdu, 610065, China.

[b] Institute for Applied Materials (IAM), Karlsruhe Institute of Technology (KIT), Hermann-von-Helmholtz-Platz 1, 76344 Eggenstein-Leopoldshafen, Germany.

[c] College of Materials Science and Engineering, Chongqing University, Chongqing 400030, China.

[d] School of Chemical Engineering and Technology, Xi'an Jiaotong University, Xi'an,710049, China.

[e] Institute for Advanced Study, Chengdu University, Chengdu, 610106, China.

[f] Chemistry and Chemical Engineering Guangdong Laboratory, Shantou, 515041, China.

* Corresponding authors.

Email: xiaodong2009@163.com (Xiaodong Guo)

zhenguowu@scu.edu.cn (Zhenguo Wu)

METHODS:

Material synthesis: 4 mmol vanadium phosphate (VPO) or carbon-coated vanadium phosphate (c-VPO) and Sodium fluoride are mixed in a molar ratio of 1:1.575 and put into a 100 ml hydrothermal kettle, and 50 ml deionized water is added. Stir the mixture in a 30 °C water bath to mix evenly, and add trace amounts of nitric acid to regulate pH=7. The sealed reaction kettle is insulated at 180 °C for 36 hours. After the reaction is completed, wash with water 4 times and dry at 100 °C for 12 hours in a drying oven to obtain the product. The products synthesized from VPO and c-VPO are named NVPF and NVPF-(002), respectively.

Materials characterization: The morphologies of samples were observed by field emission scanning electron microscope (FESEM, JSM-7610F, JEOL Ltd., Japan) and transmission electron microscope (TEM, JEM-F200, JEOL Ltd., Japan). The powder synchrotron radiation X-ray diffraction (SRXRD) characterization was conducted at DESY (Deutsches Elektronensynchrotron, Hamburg, Germany). The original wavelength was changed to 1.54180 Å for analysis. Mix the samples with KBr and press the tablets, then use Thermo Fisher Nicolet IS10 to collect the Fourier-transform infrared spectroscopy (FTIR). Raman data was obtained on a confocal micro-Raman spectrometer (inVia, Renishaw) with a laser wavelength of 532 nm. Thermogravimetric analysis (TG, NETZSCH STA 449F3) was used to characterize the mass changes of two samples. The C1s narrow spectra were tested by X-ray photoelectron spectroscopy (XPS, Thermo Scientific K-Alpha). The ultraviolet-visible spectrophotometer (UV-vis, SolidSpec-3700, Shimadzu) was used to measure the diffuse reflectance spectra. The synchrotron X-ray absorption spectroscopy (XAS) measurement was conducted on the P64 beam line of PETRA-III in Hamburg, Germany. The absorption edge of the V foil also collects reference spectra for energy calibration. Use the Demeter software package to process XAS spectra.

Electrochemical Measurements: The active materials were mixed with the acetylene black (AB) and poly(tetrafluoroethylene) (PTFE, from canrd) binder at a mass ratio of 70:20:10. Then roll the mixture to prepare an electrode film with a mass load of ~3 mg

cm^{-2} for the active material. The prepared electrode film is cut into the wafer with a diameter of 10 mm as the cathode electrode. The cathode electrodes were assembled into CR 2025 coin-type cells with sodium foil as the counter electrode and glass fiber as the separator. For the preparation of hard carbon anode, mixing the hard carbon, carbon black (super C65), carboxymethyl cellulose sodium (CMC), and styrene-butadiene rubber (SBR) in deionized water in the mass ratio of 80: 10: 5: 5. After that, the slurry was evenly coated on the copper foil and dried at 110°C under vacuum for 6 h. The electrolyte used in the present work consisted of 1 M $NaClO_4$ in propylene carbonate (PC) and ethylene carbonate (EC) (1:1, v:v) with 5% fluoroethylene carbonate (FEC). CR 2025 coin-type cells for half-cell, CR2032 coin-type cells for full cell were fabricated in an argon-filled glove box with the water and oxygen contents kept at less than 0.1 ppm. The galvanostatic charge/discharge measurements were performed using a Neware battery testing system (CT-4008T). The voltage window between 2.0 and 4.5 V (vs Na/Na^+) was selected, and 1 C = 128 mA g^{-1}. Galvanostatic intermittent titration technique (GITT) measurement for obtaining Na^+ diffusion coefficient. Cyclic voltammetry (CV, 2-4.5 V, 0.15 mv s^{-1}) measurements were performed on a CHI760D electrochemical workstation.

Computational method 1: We have employed the Vienna Ab Initio Package (VASP) to perform all the density functional theory (DFT) calculations within the generalized gradient approximation (GGA) using the PBE formulation. We have chosen the projected augmented wave (PAW) potentials to describe the ionic cores and take valence electrons into account using a plane wave basis set with a kinetic energy cutoff of 400 eV. Partial occupancies of the Kohn−Sham orbitals were allowed using the Gaussian smearing method and a width of 0.05 eV. The electronic energy was considered self-consistent when the energy change was smaller than 10^{-5} eV. A geometry optimization was considered convergent when the force change was smaller than 0.02 eV/Å. Grimme's DFT-D3 methodology was used to describe the dispersion interactions.

The equilibrium lattice constants of the tetragonal $Na_3V_2(PO_4)_2F_3$ unit cell were

optimized to be a=9.080 Å, c=10.670 Å. We then use it to construct 4 surface models. The first two are Na-terminated and V-terminated $Na_3V_2(PO_4)_2F_3(001)$ surface models (models 1 and 2) with *p* (2×2) periodicity in the X and Y directions and one stoichiometric layer in the Z direction separated by a vacuum layer in the depth of 20 Å to separate the surface slab from its periodic duplicates. During structural optimizations, the Γ point in the Brillouin zone was used for k-point sampling, and the bottom half stoichiometric layer was fixed while the top half was allowed to relax. The second two models are Na-terminated and V-terminated $Na_3V_2(PO_4)_2F_3(110)$ surface models (models 3 and 4) with *p* (2×1) periodicity in the X and Y directions and one stoichiometric layer in the Z direction separated by a vacuum layer in the depth of 20 Å to separate the surface slab from its periodic duplicates. During structural optimizations, a 1×2×1 k-point grid in the Brillouin zone was used for k-point sampling, and the bottom stoichiometric layer was fixed while the top one was allowed to relax.

The adsorption energy (E_{ads}) of adsorbate carbon cluster (c-cluster) was defined as:

$$E_{ads} = E_{A/surf} - E_{surf} - E_{A(g)}$$

where $E_{A/surf}$, E_{surf}, and $E_{A(g)}$ are the energy of c-cluster adsorbed on the surface, the energy of clean surface, and the energy of c-cluster in a cubic periodic box with a side length of 20 Å and a 1×1×1 Monkhorst-Pack k-point grid for Brillouin zone sampling, respectively.

Computational method 2: Spin-polarized DFT calculations were performed using the Vienna ab initio simulation package (VASP). The generalized gradient approximation proposed by Perdew, Burke, and Ernzerhof (GGA-PBE) is selected for the exchange-correlation potential. The K-points of 221 was employed and energy cutoff was set to 400 eV. The pseudo-potential was described by the projector-augmented-wave (PAW) method. The geometry optimization is performed until the Hellmann–Feynman force on each atom is smaller than 0.02 $eV \cdot Å^{-1}$. The energy criterion is set to 10^{-6} eV in iterative solution of the Kohn-Sham equation. CI-NEB method is used to obtain the diffusion energy barrier.

Additional results

Table S1 Crystallographic data of NVPFs obtained from Rietveld refinements.

Samples			NVPF-(002)	NVPF
$Na_3V_2(PO_4)_2F_3$		*a*	9.04653	9.04549
Lattice parameters [Å]		*b*	9.04653	9.04549
		c	10.74423	10.74936
Cell volume [Å^3]			879.3	879.5
Weight fraction (wt.%)	$Na_3V_2(PO_4)_2F_3$		99.0	97.2
	VPO_4		1.0	2.8
Reliability factors(%)	R		9.74	8.12
	E		5.69	6.31

Table S2 The atomic position and occupation of the NVPF-(002)

Atom	Wyckoff positions	x	y	z	B_{iso}	Occupancy
Na1	8i	0.5234	0.2299	0	6.60562	1
Na2	8i	0.803	0.0512	0	0.58324	1/2
V1	8j	0.24783	0.24783	0.18845	0.0	1
P1	4d	0	1/2	1/4	0.0	1
P2	4e	0	0	0.2553	0.0	1
O1	16k	0.0969	0.4059	0.1629	0.04632	1
O2	8j	0.0947	0.0947	0.1682	0.0	1
O3	8j	0.4031	0.4031	0.1605	0.0	1
F1	4f	0.2476	0.2476	0	2.3715	1
F2	8j	0.2466	0.2466	0.3642	1.07412	1

Table S3 The atomic position and occupation of the NVPF.

Atom	Wyckoff positions	x	y	z	B_{iso}	Occupancy
Na1	8i	0.5234	0.2299	0	7.2679	1
Na2	8i	0.803	0.0512	0	0.0	1/2

V1	8j	0.24783	0.24783	0.18845	1.39252	1
P1	4d	0	1/2	1/4	0.0	1
P2	4e	0	0	0.2553	0.74542	1
O1	16k	0.0969	0.4059	0.1629	4.2624	1
O2	8j	0.0947	0.0947	0.1682	0.17641	1
O3	8j	0.4031	0.4031	0.1605	0.0	1
F1	4f	0.2476	0.2476	0	6.0835	1
F2	8j	0.2466	0.2466	0.3642	2.01544	1

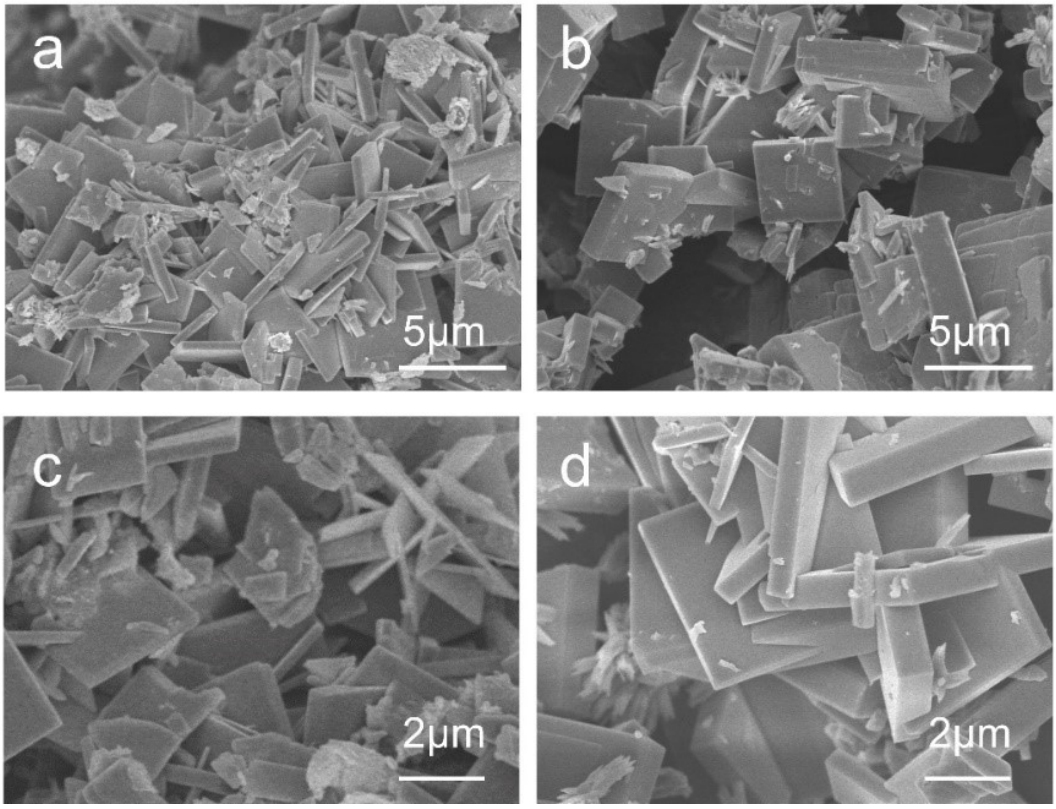

Figure S1 SEM images at different magnifications: (a), (c) NVPF-(002); (b), (d) NVPF.

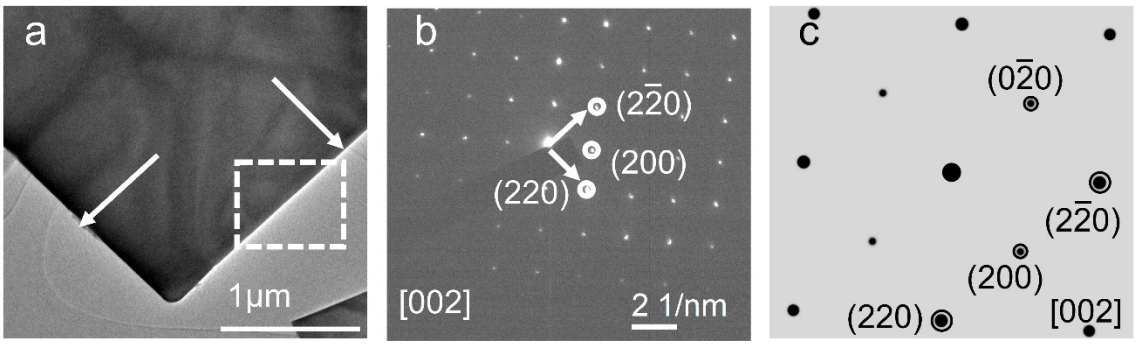

Figure S2 (a) The surface TEM image. (b) SAED pattern. (c) Simulated electron diffraction pattern of [001] zone axis.

Supporting Text 1:

As shown in **Figure S3**, in a rectangular particle, length, width, and thickness are defined as a, b, and c, respectively. The top and bottom surfaces are (002) crystal facets, and the four sides are (220) crystal facets. So, the area of (002) crystal facets is calculated by the formula $S_{(002)}$=(a*b)*4. Similarly, the area of (220) crystal facets is calculated using the formula $S_{(220)}$=(a*c)*2+(b*c)*2. The total area is calculated by the formula $S_{total}=S_{(002)}+S_{(220)}$. The exposure ratios of (002) and (220) crystal facets are calculated by $S_{(002)}/S_{total}$ and $S_{(220)}/S_{total}$, respectively. The average particle size of NVPF-(002) and NVPF samples is shown in **Table S4**.

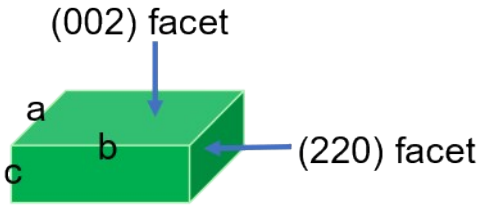

Figure S3 Schematic diagram of particle shape parameters.

Table S4 Average particle size of NVPF-002 and NVPF samples.

	a-Length (nm)	b-Width (nm)	c-Thickness (nm)	Crystal Facets Exposure Ratio (%)	
				(002)	(220)
NVPF-(002)	3063	3063	327	82	18
NVPF	3062	3062	774	66	34

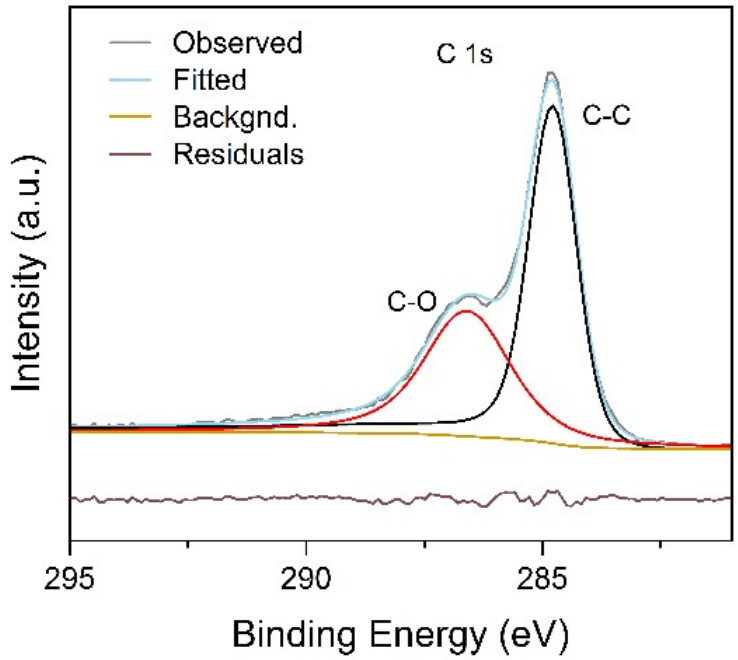

Figure S4 XPS Spectra of C1s in carbon clusters.

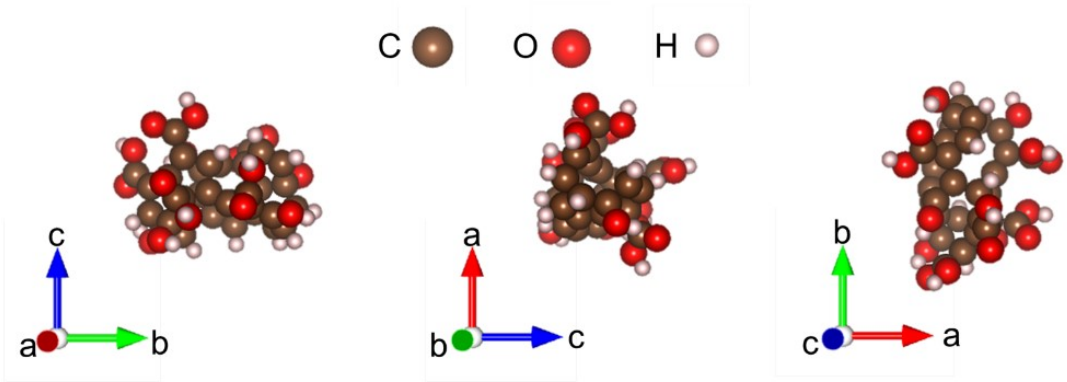

Figure S5 Atomic structure of the c-cluster.

Table S5 Atomic Coordinates and Structure Parameters of c-cluster.

	x	y	z	Occ.	U	Site	Sym.
C1	0.41088	0.56982	0.37112	1.000	0.000	1a	1
C2	0.46727	0.69713	0.36892	1.000	0.000	1a	1
C3	0.59796	0.54914	0.44191	1.000	0.000	1a	1
C4	0.58302	0.40682	0.45377	1.000	0.000	1a	1
C5	0.48537	0.40762	0.34337	1.000	0.000	1a	1

C6	0.43711	0.63287	0.41239	1.000	0.000	1a	1
C7	0.44777	0.64710	0.48631	1.000	0.000	1a	1
C8	0.57668	0.48906	0.47449	1.000	0.000	1a	1
C9	0.39903	0.50214	0.40181	1.000	0.000	1a	1
C10	0.41807	0.42263	0.39557	1.000	0.000	1a	1
C11	0.45408	0.60445	0.55997	1.000	0.000	1a	1
C12	0.47587	0.72607	0.49970	1.000	0.000	1a	1
C13	0.54814	0.49150	0.56244	1.000	0.000	1a	1
C14	0.50019	0.30868	0.49163	1.000	0.000	1a	1
C15	0.54977	0.71690	0.37345	1.000	0.000	1a	1
C16	0.55038	0.37078	0.38151	1.000	0.000	1a	1
C17	0.49290	0.75635	0.42259	1.000	0.000	1a	1
C18	0.61733	0.68352	0.40589	1.000	0.000	1a	1
C19	0.53131	0.71371	0.56138	1.000	0.000	1a	1
C20	0.63591	0.61425	0.43442	1.000	0.000	1a	1
C21	0.54405	0.36653	0.51792	1.000	0.000	1a	1
C22	0.55448	0.41043	0.58268	1.000	0.000	1a	1
C23	0.49738	0.30836	0.40839	1.000	0.000	1a	1
C24	0.40745	0.46159	0.46707	1.000	0.000	1a	1
C25	0.43066	0.34686	0.36311	1.000	0.000	1a	1
C26	0.51615	0.65011	0.59693	1.000	0.000	1a	1
C27	0.47055	0.52171	0.56079	1.000	0.000	1a	1
C28	0.41690	0.46580	0.54267	1.000	0.000	1a	1
C29	0.38008	0.62031	0.60111	1.000	0.000	1a	1
C30	0.66784	0.39157	0.45757	1.000	0.000	1a	1
C31	0.71355	0.60702	0.46769	1.000	0.000	1a	1
C32	0.44663	0.26136	0.52844	1.000	0.000	1a	1
C33	0.57020	0.38636	0.65712	1.000	0.000	1a	1
H1	0.58552	0.52820	0.59371	1.000	0.000	1a	1

H2	0.56547	0.75166	0.32579	1.000	0.000	1a	1
H3	0.48803	0.44306	0.29417	1.000	0.000	1a	1
H4	0.48126	0.81506	0.41344	1.000	0.000	1a	1
H5	0.54196	0.63086	0.64820	1.000	0.000	1a	1
H6	0.57165	0.75511	0.57940	1.000	0.000	1a	1
H7	0.44100	0.71161	0.31618	1.000	0.000	1a	1
H8	0.40952	0.57500	0.31065	1.000	0.000	1a	1
H9	0.50894	0.25490	0.38127	1.000	0.000	1a	1
H10	0.37973	0.36921	0.56679	1.000	0.000	1a	1
H11	0.65623	0.78316	0.39784	1.000	0.000	1a	1
H12	0.63952	0.38105	0.31980	1.000	0.000	1a	1
H13	0.35753	0.27163	0.35052	1.000	0.000	1a	1
H14	0.40464	0.76030	0.57618	1.000	0.000	1a	1
H15	0.27932	0.59143	0.60493	1.000	0.000	1a	1
H16	0.75721	0.42192	0.40910	1.000	0.000	1a	1
H17	0.76187	0.60996	0.56116	1.000	0.000	1a	1
H18	0.41451	0.22043	0.61937	1.000	0.000	1a	1
H19	0.59009	0.42341	0.75332	1.000	0.000	1a	1
O1	0.40107	0.41272	0.59193	1.000	0.000	1a	1
O2	0.67449	0.73369	0.41052	1.000	0.000	1a	1
O3	0.60329	0.34206	0.33066	1.000	0.000	1a	1
O4	0.38339	0.30683	0.31806	1.000	0.000	1a	1
O5	0.41859	0.77639	0.52602	1.000	0.000	1a	1
O6	0.37110	0.67025	0.64624	1.000	0.000	1a	1
O7	0.32410	0.57569	0.57812	1.000	0.000	1a	1
O8	0.69996	0.35364	0.50292	1.000	0.000	1a	1
O9	0.70372	0.42975	0.40224	1.000	0.000	1a	1
O10	0.76957	0.59064	0.43379	1.000	0.000	1a	1
O11	0.71118	0.61778	0.54254	1.000	0.000	1a	1

O12	0.39547	0.22976	0.49424	1.000	0.000	1a	1
O13	0.45364	0.25490	0.60357	1.000	0.000	1a	1
O14	0.58097	0.32253	0.67894	1.000	0.000	1a	1
O15	0.57559	0.44625	0.70613	1.000	0.000	1a	1

Table S6 Calculated surface energy of different layers.

Layer	E_{surf} (eV)	E_{bulk} (eV)	Area (Å^2)	Surface Energy (eV Å^2)
V-P layer	-433.58	-446.81	163.48	0.08
Na-F layer	-493.43	-502.31	163.48	0.05
V-P-O layer	-621.11	-647.87	274.78	0.10
Na-O layer	-543.11	-559.45	274.78	0.06

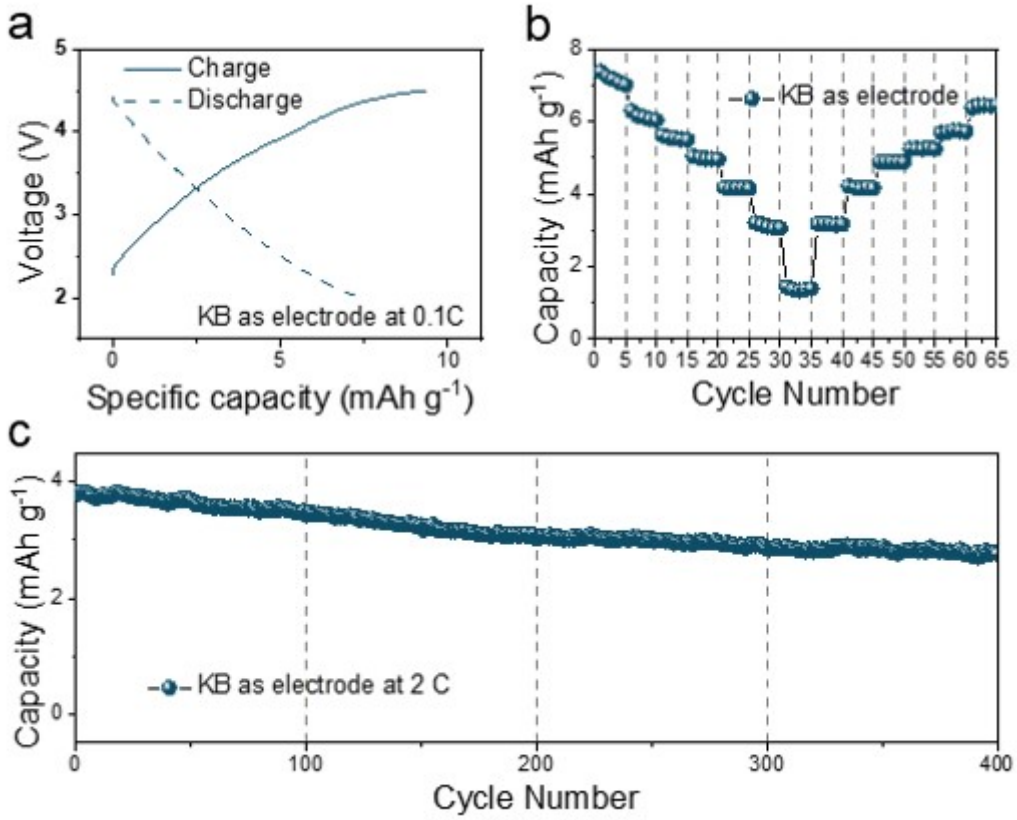

Figure S6 Electrochemical measurement at room-temperature: (a) Charge-discharge curves of KB as electrode at 0.1 C. (b) Rate performance of KB electrode at 0.1 C, 0.2 C, 0.3 C, 0.5 C, 1 C, 2 C,

and 5 C. (c) Cycle performance of KB electrode at 2 C. The specific capacity is the contribution of KB to the specific capacity of NVPFs electrodes.

Table S7 Specific results of electrochemical performance of NVPF-(002)/NVPF cathode.

		Rates						
		0.1 C	0.2 C	0.3 C	0.5 C	1 C	2 C	5 C
NVPF-(002)	Specific capacity mAh g^{-1}	132	131	130	128	126	122	98
NVPF		123	124	124	121	114	89	58
NVPF-(002)	Power density W kg^{-1}	46	94	156	231	455	890	2123
NVPF		46	94	154	228	443	853	2007
NVPF-(002)	Energy density Wh kg^{-1}	482	478	474	467	453	425	338
NVPF		451	458	451	434	396	318	175

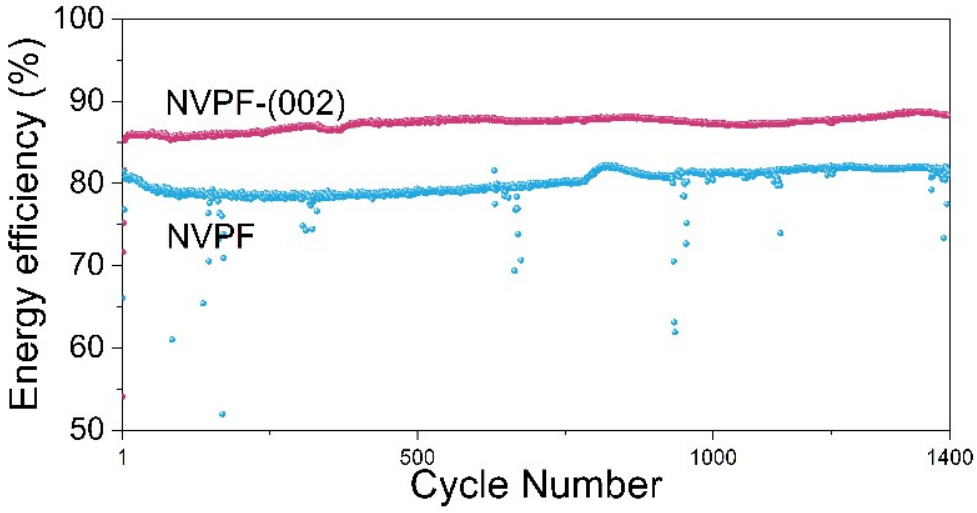

Figure S7 Energy efficiency comparison of NVPFs cathodes.

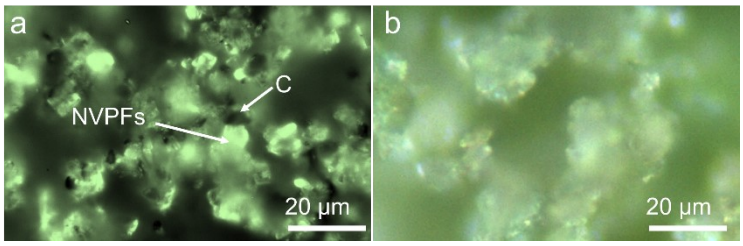

Figure S8 Optical microscope image: (a) NVPF-(002) sample, (b) NVPF sample.

Table S8 The conductivity comparison between two samples assembled into electrode plates.

Sample	Voltage (mV)	Resistance (Ω)	Resistivity (Ω mm)	Conductivity (S mm^{-1})
NVPF-(002)	+36.4917	36.4917	5.47525	0.182640
	-36.4821	36.4821	5.47549	0.182632
NVPF	+36.4881	36.4881	5.47451	0.182665
	-36.4715	36.4715	5.47295	0.182717

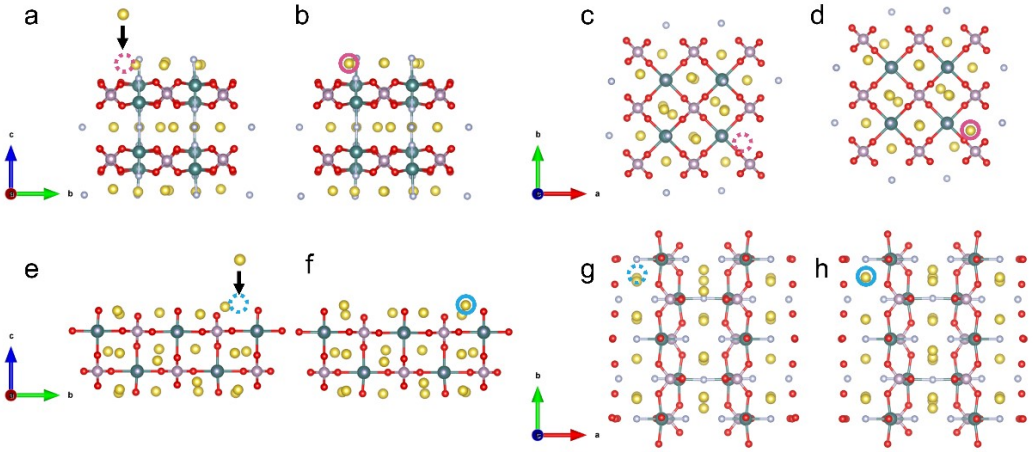

Figure S9 Na^+ binding sites on different facets:(a-d) (001) facet (red), (e-h) (110) facet (blue).

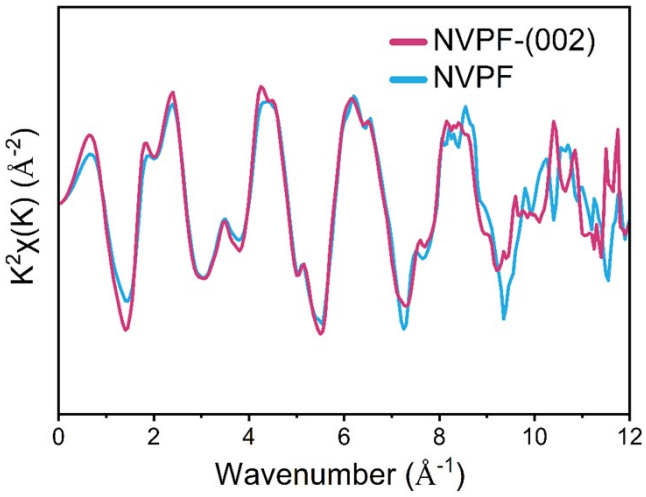

Figure S10 K-space quadratic weighted signal.

Table S9 Bond length parameters for each bond in VO_4F_2 octahedron in NVPF-(002) sample.

From atom	x, y, z	To atom	x, y, z	Bond length (Å)
V1	(0.248,0.248,0.188)	F1	(0.248,0.248,0.0)	2.0248
V1	(0.248,0.248,0.188)	F2	(0.247,0.247,0.364)	1.8884
V1	(0.248,0.248,0.188)	O1	(0.406,0.097,0.163)	1.9961
V1	(0.248,0.248,0.188)	O1	(0.097,0.406,0.163)	1.9961
V1	(0.248,0.248,0.188)	O2	(0.095,0.095,0.168)	1.9711
V1	(0.248,0.248,0.188)	O3	(0.403,0.403,0.161)	2.0091

Table S10 Bond length parameters for each bond in VO_4F_2 octahedron in NVPF sample.

From atom	x, y, z	To atom	x, y, z	Bond length (Å)
V1	(0.248,0.248,0.188)	F1	(0.248,0.248,0.0)	2.0257
V1	(0.248,0.248,0.188)	F2	(0.247,0.247,0.364)	1.8893
V1	(0.248,0.248,0.188)	O1	(0.406,0.097,0.163)	1.9959
V1	(0.248,0.248,0.188)	O1	(0.097,0.406,0.163)	1.9959
V1	(0.248,0.248,0.188)	O2	(0.095,0.095,0.168)	1.9709
V1	(0.248,0.248,0.188)	O3	(0.403,0.403,0.161)	2.0088

Table S11 the radial distance difference between NVPF-002 and NVPF.

From atom	To atom	NVPF-(002) Bond length (Å)	NVPF Bond length (Å)	Radial distance difference (Å)
V1	F1	2.0257	2.0257	-0.0009
V1	F2	1.8893	1.8893	-0.0009
V1	O1	1.9959	1.9959	0.0002
V1	O1	1.9959	1.9959	0.0002
V1	O2	1.9709	1.9709	0.0002
V1	O3	2.0088	2.0088	0.0003

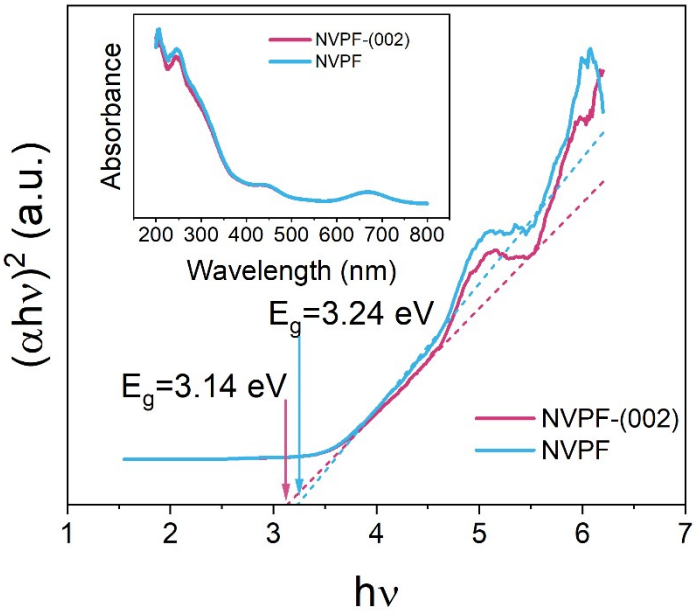

Figure S11 Plots of $(\alpha h\nu)^2$ versus $(h\nu)$ for obtaining the Eg of NVPF-(002) and NVPF. Insert image: UV-vis diffuse reflectance absorption spectra of NVPF-(002) and NVPF.

Supporting Text 2:

The assembled battery was discharged/charged for 10 cycles within a voltage range of 2.0-4.5 V vs. Na/Na^+ and a current density of 1 C (to obtain a steady state) and then the battery was charged to 2.0 V for galvanostatic intermittent titration technique (GITT) measurement. Subsequently, the discharge current is maintained constant for 600 s, and

then the discharge current is interrupted for 3600 s to allow relaxation to return to equilibrium. Repeat the above process until the battery is fully discharged.

The D_{Na^+} can be calculated via the formula (1) from the reported methodology.[51, 52]

$$D_{Na^+} = \frac{4}{\tau\pi}\left(\frac{n_M V_M}{A}\right)^2 \left(\frac{dE_s}{dE_\tau}\right)^2 \quad (1)$$

Where dE_τ and dE_s are the voltage variations in constant current discharge and pulse in a single-step GITT measurement, respectively. τ is the relaxation time. The definition of dE_τ, dE_s, and τ is marked in the Figure S12. n_M and V_M are the moles (mol) and molar volume. A is the electrode-electrolyte interfacial area (cm^2).

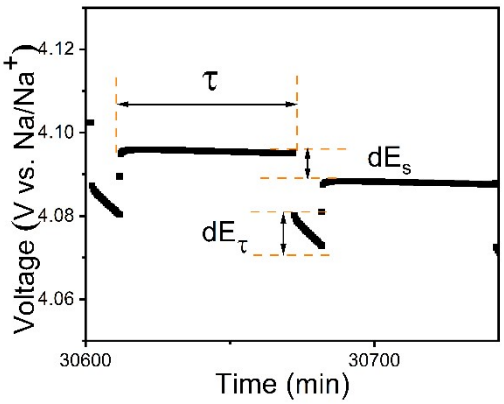

Figure S12 The voltage vs. time curve of single GITT titration and definition of dEτ, dEs, and τ.

Table S12 Oxidation-reduction potential and potential difference of NVPFs.

sample	Anodic peak (V)	Cathodic peaks (V)	Potential difference(V)
NVPF-(002)	3.85	3.43	0.42
	4.35	3.95	0.40
NVPF	3.97	3.35	0.62
	4.43	3.83	0.6

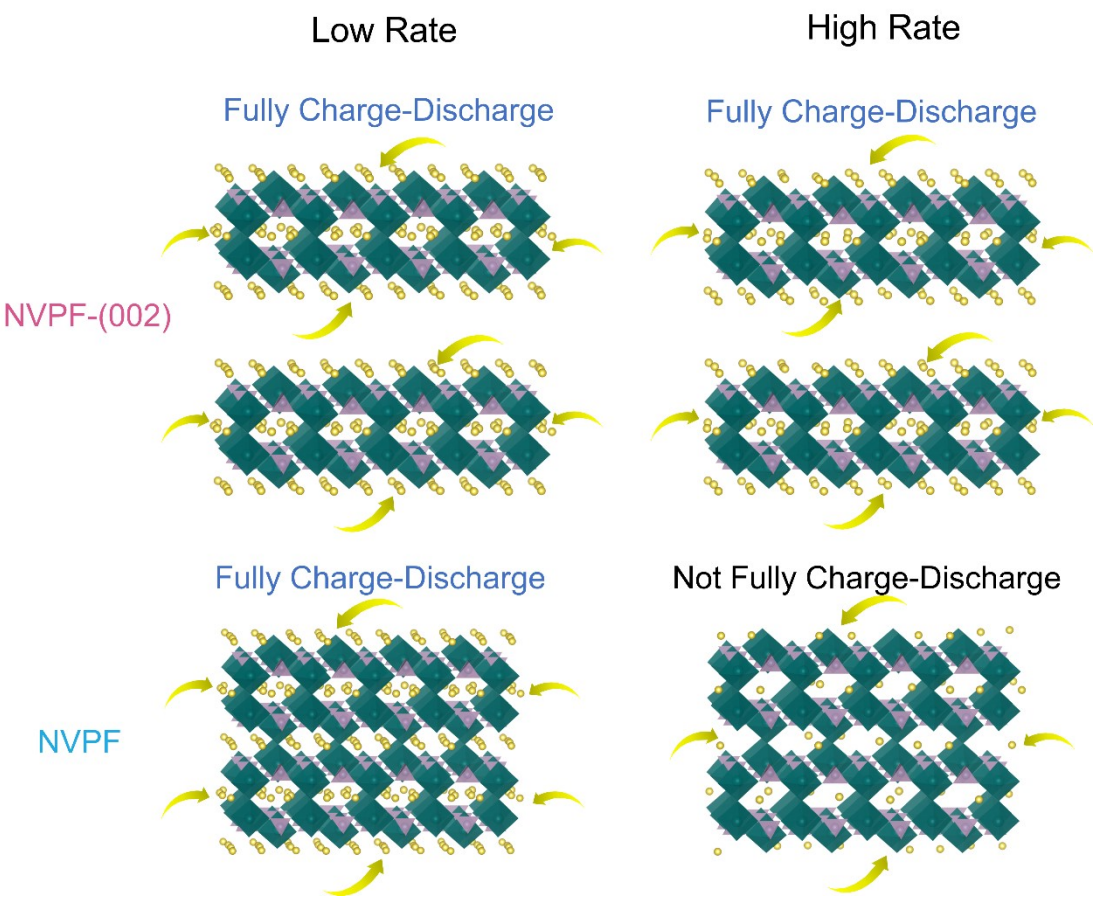

Figure S13 Schematic illustrating of Na^+ storage mechanism at low and high rate.